GAS CHIMNEYS: An Effective Exploration Tool

Fred Aminzadeh, dGB-USA, Tim Berge, Forest Oil, Paul de Groot, dGB BV, Guiseppe Valenti, Agip

Summary

Long before the discovery of hydrocarbons in the middle of 19th century, seepage of oil and gas to the surface of the earth was evidenced in different hydrocarbon-rich areas of the world. Temples of fire worshippers with their “eternal flames” began to canvass many population centers long times ago. Fire raged from “Atashkadeh”s of Zorostarians of ancient Persia to those of Aztecs in South America. Those fires, for the most part, were fueled by the natural gasses that were seeping from different sub-surface accumulations through “gas chimneys”. Some of these sites, such as the one just outside Baku, continue to be in operation.

Several thousand years later, likes of Drake in the US, Darcy in Iran and Nobel in Azerbaijan used in part information from such surface seepage to drill successful oil wells and opening a new chapter in industrial revolution. Before the introduction of gravity, magnetic and seismic methods, natural hydrocarbon seepage and the corresponding surface evidence continued to be the most common tool for exploration. As a result, most major oil fields discovered in the first 60 years of oil industry were close to known seepage locations. It is no accident that many smaller fields pre-dated discovery of the largest oil field in the world, Ghawar. Indeed, absence of such seepage in the deserts of Saudi Arabia was what prompted Sir Jon, the English explorer’s proclamation: “I would drink all the oil in this land to the last drop if any were found here”!

Surface geochemistry methods developed in the last thirty years analyze concentrations of natural gas in the air or from sea water or soil samples. This allows detection of more subtle seepage with limited foot-prints. Likewise, one can see evidence of gas clouds or mud volcanoes from chaotic behavior of seismic character. As advanced geochemical methods push the limits of detection of slight evidence of hydrocarbon from outcrops and soil samples, so does the newly introduced gas chimney cube detect more subtle gas clouds. Chimney cubes, combined with other features such as pockmarks, surface evidence of mud-volcanoes, remote sensing data and structural/stratigraphic models can be used as a powerful tool.

This paper will highlight only some of the applications of this new technology. Among those are: unraveling a basin’s hydrocarbon history, establishing the migration path, distinguishing between charged and non-charged prospects or sealing versus non sealing faults, identifying potential for over-pressure and detecting geo-hazards

The Concept. / Procedure

Here a new concept (seismic entity,) is introduced that will be called chimney cube. A chimney cube is a 3D volume of seismic data, which highlights vertical chaotic behavior of seismic characters. These disturbances are often associated with gas chimneys. The cube facilitates the difficult task of manual interpretation of gas chimneys. It reveals information on the hydrocarbon history, migration paths and fluid flow models. Practically, chimney cubes can reveal where hydrocarbons were originated, how they migrated into a prospect and how they spilled from this prospect and or created shallow gas, mud volcanoes or pock marks at the sea bottom. As such a chimney cube can be seen as a new indirect hydrocarbon indicator tool. Through this process, a seismic volume (and corresponding attributes) are provided as input to a neural network and a chimney cube is generated as its output (Figure 1).

The procedure involves: 1) calculating and identifying a set of single-trace and multi-race seismic attributes that distinguish between chimneys and non chimneys, 2) designing and training a neural network with attributes extracted at interpreted chimneys and non chimney locations.3) Creating a “chimney cube” volume from multi-attribute transformation of the 3D seismic volume highlighting vertical disturbances as the output of the trained neural network, 4) visualizing and interpreting the chimney volume. Using the chimney cube in conjunction with other structural, stratigraphic and geophysical interpretations of acoustic impedance, AVO, and fluid factor allows us to study chimneys as the spatial link between source rock, reservoir trap, spill-point and shallow-gas anomalies.

Attribute extraction

Based on prior experience and geology of the area an intelligent selection of attributes that have potential to increase the contrast between chimneys and non chimneys are made. Attributes can be amplitude, energy, similarity, frequency, phase, dip, and azimuth among others. For additional details and definition of these and other attributes see Aminzadeh (1990). Moreover, attributes can be extracted (and merged) from different input cubes e.g. near - and far offset stack, inverted acoustic impedance etc. Many of these attributes are influenced by the shape and orientation of the extraction window. Figure 2A shows the attribute extraction window, (actually an extraction volume). The vertically oriented extraction volume reflects the fact that in chimney detection we are looking for vertically oriented bodies of considerable dimensions. We use knowledge about the characteristics of chimneys by calculating in each extraction volume such attributes as energy and various types of trace-to-trace similarity. Note that for fault detection, dipping windows and for reflector detection horizontally oriented windows (Figure 2B and 2C) would be used. Finally, a window (volume) such as the one in Figure 2D would be used to highlight a more general geologic body. Such an extraction volume follows the desired object at every position. This implies that the extraction volume has a flexible shape, which follows the local dip and azimuth of the data. The local dip and azimuth can be calculated in many different ways. We use a modified version of the Wigner-Radon transformation scheme developed by Steeghs (1997). We found that the calculated local dip and azimuth cannot only be used to steer the attribute extraction volumes but it is also a perfect vehicle to remove random noise prior to attribute extraction processes.

The attributes constituting the input of the neural network (to be discussed in the next section) are calculated as follows:

1) Reference Time is the time in ms. of the sample position at which the attributes are extracted.

2) Energy gate is the energy calculated in a time gate between A and B ms. relative to the reference time. Energy is calculated as the integration over the square of the amplitudes, divided by the number of samples.

3) Dip Angle Variance is the variance of the angle of the dip of all samples inside a time gate and a block vertex size of 2*N+1 traces (N is referred to as the trace step out). The dip is calculated with a sliding Fourier-Radon transform (Tingdahl, 1999). The angle is the angle between the local seismic direction and a horizontal plane. It is calculated within an optional step-out

4) Similarity Measure is the similarity between two trace pairs and those same pairs after rotation by 90 degrees. The reference trace is called 0,0. Trace 1,1 is the neighbouring trace located in the upper right quadrant. 'value=Average' will output the average of these two values, 'value=Minimum' will output the minimum of the two values.

Similarity is defined as:

$$S = 1 - \Sigma[(s_{1,i}-s_{2,i})^2] / (\Sigma [s_{1,i}^2] + \Sigma[s_{2,i}^2])$$

where Σ is the summation over the samples in the specified time gate. If trace samples are considered a vector in hyper-space, then similarity is one minus the length of the difference vector divided by the sum of the lengths. This value is always between 0 and 1.

Time gate [A,B] is defined on the reference trace. To find the corresponding time gate [A',B'] on the traces at pos1, pos2 and the 90 degrees rotated trace pair we follow the local dip and azimuth from the reference position in the direction of the target traces. This process is called steering. Full-steering means that we follow the dip from trace to trace until we reach the target trace. We also use an option to fine tune the reference time on the target trace by searching for the same signal phase on the target trace as compared to the starting position. It is turned on in situations where noise levels are very low.

A key step in the procedure is that attributes are extracted in three separate time windows: one above, one at and one below the point of investigation. In this way we utilize the knowledge that chimneys are vertical bodies with a certain dimension. Most time-windows in this network have a length of 80ms some have 40ms lengths. It should be emphasized that combining different attributes through the training process help distinguishing chimneys from other non-vertical disturbances. Figure 3 demonstrates this fact by comparing chimneys identified by a multitude of attributes (Figure 3A) with a single-attribute output of coherency (Figure 3B) which does not separate chimneys from other disturbances.

Neural networks

Neural networks have recently gained much popularity in different petroleum industry applications. Typically, neural networks can be considered as a non linear transformation between its input parameters and the desired output. The main feature of these networks is the fact that one does not attempt to derive the explicit nonlinear relationship (unlike what is done in conventional regression analysis). Instead, a collection of optimum weights is derived to relate the output of the nodes to their input using the available information (data). These weights, combined with the intrinsic nonlinear (sigmoid) functions define each node, creating the implicit nonlinear functions between the input and output of the entire network. Figure 4 shows a schematic neural network where a non-linear mapping of input variables x1 and x2 (say two selected seismic attributes) yields the output y through an implicitly-derived multi-dimensional non-linear function.

In our chimney application, after the selected attributes have been extracted at a representative set of data points we will recombine these into a new set of attributes to facilitate the detection process. In this step we use supervised and unsupervised neural networks.

The main difference between the supervised and unsupervised learning approach lies in the amount of a-priori information that is supplied. Supervised learning requires a representative set of examples to train the neural network. For example networks can be trained to find the (possibly non-linear) relation between seismic response and the rock property of interest (e.g. de Groot, 1999a and b). In this case the training set is constructed from real or simulated well data. In unsupervised (or competitive learning) approaches, the aim is to find structure within the data and thus extract relevant properties, or features. The resulting data segments (patterns) still need to be interpreted. An example of this approach is the popular wave-form segmentation method whereby wave-forms along an interpreted horizon are segmented. The resulting patterns are then interpreted in terms of facies- or fluid changes.

In the object detection method we use the same principles. If we employ unsupervised learning approaches we use attributes related to the objects we would like to detect. With the supervised learning approach we go one step further. Not only do we use meaningful attributes, we also identify locations in the seismic cube where examples of the class of objects to be detected are present. Seismic attributes are calculated at these positions as well as at control points outside the objects. The neural network is then trained to classify the input location as falling inside or outside the object. Application of the trained network yields the desired texture enhanced volume in which the desired objects can be detected more easily.

Figure 5 shows the structure of a MLP neural network with different attributes calculated from the seismic data at different time gates as its input and a measure of the combined chimney-like behavior of theses attributes as an output. Figure 6A shows the discrimination power of the attributes. At the training stage appropriate weights for the input parameters and the hidden layers (the layers of neural network involving the nodes between the input and the output) are calculated. As these weights stabilize (as manifested by the convergence in Figure 6B) we stop the training process. The optimal position to stop training is determined by monitoring the network's performance on an independent test data set (the blue curve in Figure 6B). Finally, with an acceptable level of per cent correct classification (Figure 6C), the network performs the volume transformation for the entire data set. The following steps summarize the procedure:

1. A seed interpretation is made with locations inside manually interpreted chimneys and in a control set outside the chimneys (Figure 5, the picks in yellow and red).
2. At the seed locations various energy and similarity attributes are extracted in three vertically aligned extraction volumes around the location.
3. Step 1 and 2 are repeated to create an independent test set.
4. A fully connected Multi-Layer-Perceptron type of neural network is trained to classify the attributes into two classes representing chimney or non-chimney (output vectors 1,0 or 0,1). Figure 5 shows a typical network topology.
5. The trained network is applied to the entire data set yielding outputs at each sample location. As the outputs are complementary we pass only the output on the chimney node to produce the final result: a cube with values between approx. 0 (no-chimney) and 1 (chimney), see Figure 1.

What do chimneys look like?

On seismic data chimneys appear as vertical bodies of varying dimensions. Also shape and distribution may vary, although cigar-shapes and a distribution along faulted zones are common. The internal texture shows a chaotic reflection pattern of low energy. The exact outline of a chimney is very difficult to determine on conventional seismic displays. Only large chimneys can be recognized. To also detect more subtle disturbances we have transformed the data into a new cube that highlights vertical disturbances. High values in this cube indicate a high chimney probability.

Once the chimneys are identified, they can be displayed in conjunction with other structural and reservoir property information. This helps validating certain geological interpretation such as the origination points of hydrocarbons, spill points, reservoir accumulation and gas seepage to the surface. Figure 7 is an example of such an interpretation by Heggland et.al. (2000). The deeper cloud of high amplitudes (red) corresponds to the outline of a salt dome, while the shallow cloud of high amplitudes is interpreted to represent a hydrocarbon-charged reservoir. Chimneys (yellow) surrounding the salt dome indicate upward fluid migration from a deeper reservoir. The high density of shallower chimneys indicates charging of the shallow reservoir. The subseabed surface exhibits a radial fault pattern caused by the upward movement of the salt dome. Chimneys are visible up to the seabed, and a small mound is present at the seabed close to the top of the shallowest chimney on the right-hand side. This may be a small mud volcano generated by the transport of sediments, fluid and/or gas to the seabed. The presence and distribution of the chimneys that have been mapped in this area make the presence of a deep and a shallow hydrocarbon-charged reservoir more likely.

Chimneys in South Africa

Africa has three extensive, thick, deltaic systems on it’s west coast. Of these the Congo and Niger Deltas have major commercial hydrocarbon resources. The Orange River delta is less-explored but has already had gas and oil discoveries that indicate it’s potential. These discoveries indicate that at least 3 hydrocarbon systems exist in the area; in graben deposits of the early rift succession. e.g. AJ-1 well (oil), Kudu-type late rift (gas) and in the Albian-Aptian drift succession (gas). The deepwater portion of the delta has yet to be drilled so its potential is yet to be assessed.

Here, we will focus on a 312 sq km AK 3D seismic survey in Block 2A around the AK-1 gas discovery. This allows for the first time a very detailed look at a small part of the delta. The original discovery well was plugged and abandoned as it was thought to be a small non-commercial structural trap. The 3D showed that the field, now designated the Ibhubesi Field, is in fact a giant stratigraphic trap. The 3D area may only cover a small part of the southern extent of the field, which may eventually produce as much as 15Tcf of gas. Attribute processing and gradient analyses with the chimney volume clearly show individual gas accumulations in meandering fluvial channels and other component facies of fluvial-deltaic system. Fluvial channels, meander belts, crevasse splays and overbank deposits, distributary systems and deltas can all be identified in Figure 7b which is a 3-dimensional view of the reservoir interval. Figure 8 shows a map view of this same 3D volume, but this time showing the chimney cube attribute with seepage anomalies along the main fault, both shown in red. When viewed in a vertical section, these gas seepage anomalies can be seen to originate at the reservoir level and ascend to the surface vertically.

A 4-well drilling program was undertaken to evaluate the field and prove-up a core development area with enough reserves to be economically developed. 3 different anomalies were targeted and each well will test individual compartments with 20 to 520 Mcfg per well for a total base project of 1.15 Tcfg.

To date the first three wells, have been drilled and completed. So far the results have been 100% successful. The A-K2 well tested 30 Mcfg and over 600 bbls of condensate per day from a 20 meter thick pay sand on a ¾" choke with a flowing tubing pressure of 2200 psi. The reservoir characteristics were even better than expected: clean and well sorted with average porosity of 21% (up to 25%) and almost no water saturation. There was no water produced during the test and no significant reservoir pressure draw-down seen during the 12 hr. test.

A 15m gas- bearing sand of similar quality to the A-K2 sand, but the drillstring twisted-off before drilling the second deeper sand that was subsequently penetrated successfully in a sidetrack. What is interesting about this hole so far (besides the confirmation of additional reserves) is that the lowest gas sand in the A-V1 is deeper than the lowest proven gas and highest proven water in the A-K1 well, clearly showing that this is a separate reservoir and stratigraphic trap. Bit by bit, as the well results come in, the initial vision of a giant regional stratigraphic trap is being proven.

The Chimney analysis made a significant contribution to the interpretation and validation of earlier work. Figures 9 and 10 shows how chimney analysis is integrated with the conventional seismic processing, figure 10 showing what one of the main seepage chimneys look like on a conventional reflection display. Figure 11 displays chimney output on the inline 2800 compared against the original seismic. These results were obtained after training the neural network with known and hand-picked chimneys and non-chimneys. Figure 12 displays the distribution of the number of picks from different time gates (horizontal axis shows the reference time and the vertical axis shows the number of picks from each time interval. The RMS error for the training and test data set are shown in Figure 13. Figures 14 and 15 show time slices, highlighting the major chimney like features. These features reach the sea-floor along the trace of the fault where there is a 40m meter high ridge-shaped mound formed by a chemo-tropic community of organisms that essentially live on the leaked methane gas.

Gulf of Mexico Example

The area of investigation in this case is the continental shelf-edge, western offshore Louisiana. Here thick sequences of sands and shales were deposited in outer shelf to upper slope paleo-environments. Prospective targets range in age from early Pleistocene (C. macintyrei datum) at about 13,500' sub-sea to late Pleistocene (Trimosina A datum). Both gas and oil are expected in prospective reservoirs. Several producing Pleistocene fields are found within about 6 miles of the region of investigation.

The Pleistocene depositional setting is that of a mini-basin which was created by the evacuation of a deeply-buried salt sequence. One margin of the mini-basin is cut by a north-south trending fault.

This fault system cuts the sea-floor and, on the seismic, has raised zones on the sea floor in places along its extent. Such positive features have been attributed to active sea-floor gas vents. The Chimney Cube was used to document the location and subsurface extent of probable active gas leaks. The Chimney Cube appears to provide good resolution of the vertical distribution of gas and gas saturated fluids within the 3-D volume. This distribution information was combined with structural mapping of prospective horizons in order to define hydrocarbon migration pathways and potential trapping configurations. A number of targets have been defined which lie up-dip to these zones of active vertical hydrocarbon migration.

Regionally, oil/gas production has been documented as taking place adjacent to active fluid-conductive faults, as in Eugene Island 330 Field. For this reason, documentation of active gas conduits, using the Chimney Cube, can help to define gas prospects. In this Gulf of Mexico study, seismic chimneys, which are related to hydrocarbon migration paths, are evident in the raw seismic as a vertical disturbance of the response as shown in Figure 16a. These can be attributed to hydrocarbon seepage through the subsurface, leaving a high gas saturation trail on seismic. Figure 16a shows the chaotic reflection pattern of the chimneys. Such effects, where the energy decreases, as does the trace-to-trace similarity (a kind of coherency measurement), are highlighted in Figure 16b, (methodology described earlier). Figure 17 shows the neural network chimney prediction at 1000 ms. The shape of chimneys varies considerably. Some are cylindrical (above a mound), others are elongated or curved (along fractures, faults and paleo-channels). Application of the trained network on a trace-by-trace and sample-by-sample basis yields the desired chimney prediction cube of Figure 18. A detailed display of a Figure 18 is shown in Figure 19, revealing a possible mud-volcano at the sea bottom above a seismic chimney.

Acknowledgement

The Authors acknowledge contributions of Statoil and specifically those of Roar Heggland and Paul Meldahl to the development of this technology and extensive insight and collaboration on earlier projects. Forest Oil and Agip are thanked for permission to present the data examples. Contributions of Herald Ligtenberg of dGB to gas chimney processing is also acknowledged.

References

Aminzadeh, F. Pattern Recognition and Image Processing, Geophysical Press, 1990.

Meldahl, P, Heggland, R., de Groot, P. and Bril, A. 1999. The Chimney Cube, an example of semi-automated detection of seismic bodies by directive attributes and neural networks: Part I; methodology. 69th SEG conference in Houston, 31-10-‘99 until 5-11-‘99.

Meldahl, P, Heggland, R., de Groot, P. and Bril, A. 1998. Seismic Body Recognition. Patent Application GB. 9819910.2.

Heggland, R., Meldahl, P., de Groot, P. and Aminzadeh, F., 2000. Seismic chimney interpretation examples from the Norh Sea and the Gulf of Mexico. American

Heggland, R., Meldahl, P, de Groot, P. and Bril, A. 1999. The Chimney Cube, an example of semi-automated detection of seismic bodies by directive attributes and neural networks: Part I; methodology. 69th SEG conference in Houston, 31-10-‘99 until 5-11-‘99.

de Groot, P.F.M., 1999. Volume transformation by way of neural network mapping. 61th. EAGE conference, Helsinki, 7-11 June 1999.
de Groot, P.F.M., 1999. Seismic Reservoir Characterisation Using Artificial Neural Networks. Muenster, 19th. Mintrop Seminar, 16-18 May 1999.
Tingdahl, K.M., 1999. Improving Seismic Detectability Using Intrinsic Directionality. MSc thesis Earth Science Centre Göteborg University, rep. B194 1999.

Fred Aminzadeh is president and CEO of dGB-USA. He worked for Unocal for 17years in both technical and management positions. He is the author of many books patents and articles in different aspects of geophysical technology including modeling, pattern recognition, seismic attributes, seismic data processing, AVO and reservoir characterization. He received his Ph D from University of Southern California. Aminzadeh has served as chairman of SEG research committee for two years.

Paul de Groot is co-founder and director of dGB (de Groot-Bril Earth Sciences B.V.), which specializes quantitative seismic interpretation, stratigraphic analysis, seismic inversion, neural networks-based reservoir characterization and gas chimney/fracture detection. He began his career in 1981 with Shell. He then became director of Quest Geophysical Services and subsequently served as senior geophysicist for TNO Institute of Applied Geoscience before co-founding dGB in 1995. He holds a MSc and a Ph.D. in geophysics from the University of Delft.

Giuseppe Valenti holds a M.S. degree in Geology from the Universita` of Parma, Italy, and joined Eni - A G I P Division in 1988. After few years spent in Geophysical Research and Seismic Stratigraphy Application, he moved to West Africa (Angola) and then to USA (Gulf of Mexico) to concentrate in deep water E&P.

Figure 2, A Typical chimney cube as an output of the trained network with the input seismic volume (here only a cross section of the input and output is displayed

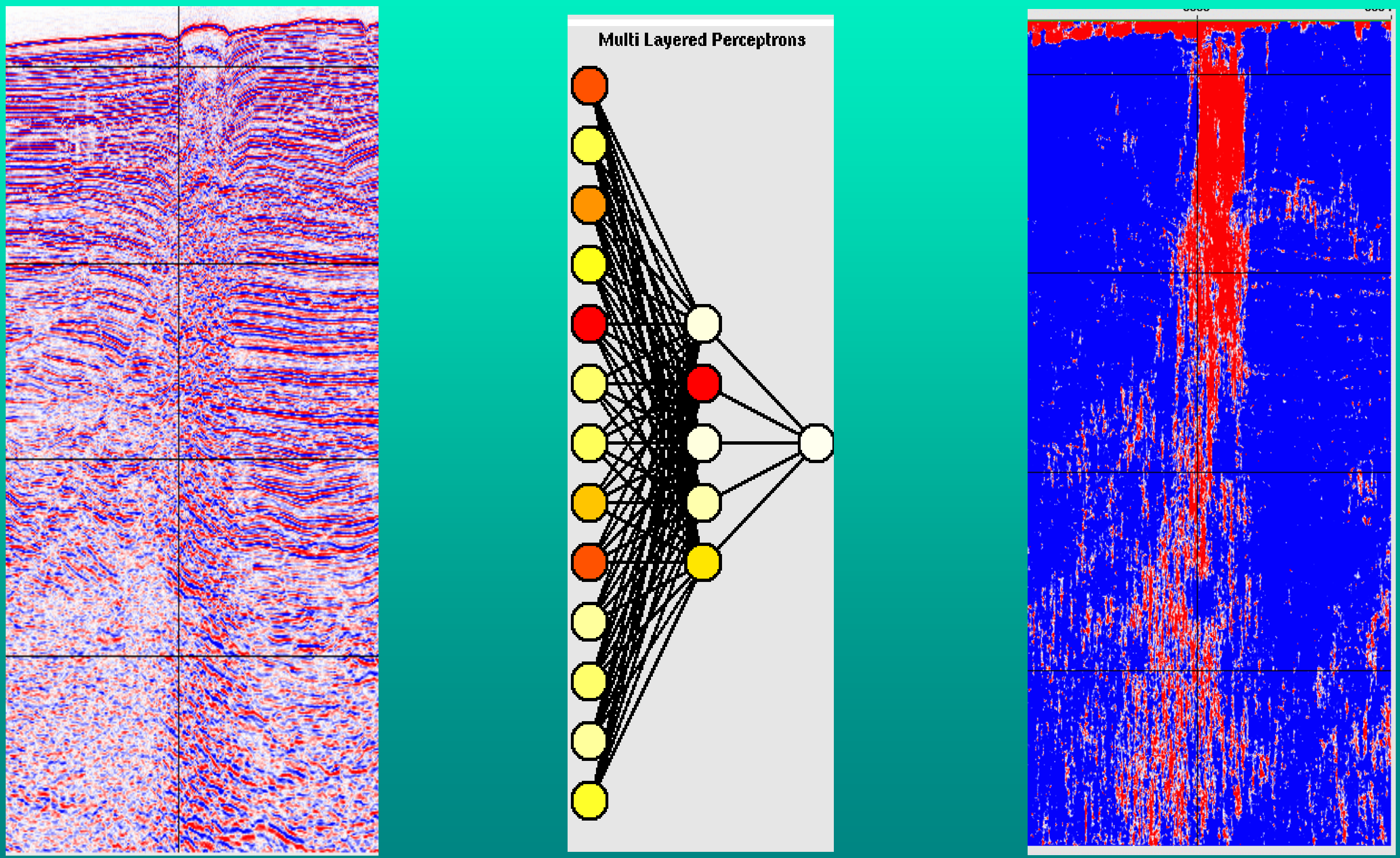

Figure 3, window (volumes) to calculate attributes:A, for chimneys, B, for bed termination, C, for faults, D general flexible bodies

Size and orientation of windows to extract attributes, or process the data follow the object we wish to detect.

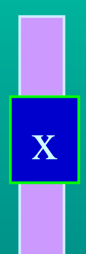

Vertical

(Chimneys)

A

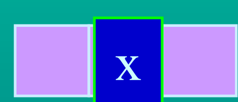

Horizontal

(Bed Termination)

B

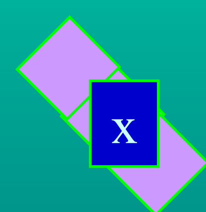

Dipping

(Faults

C

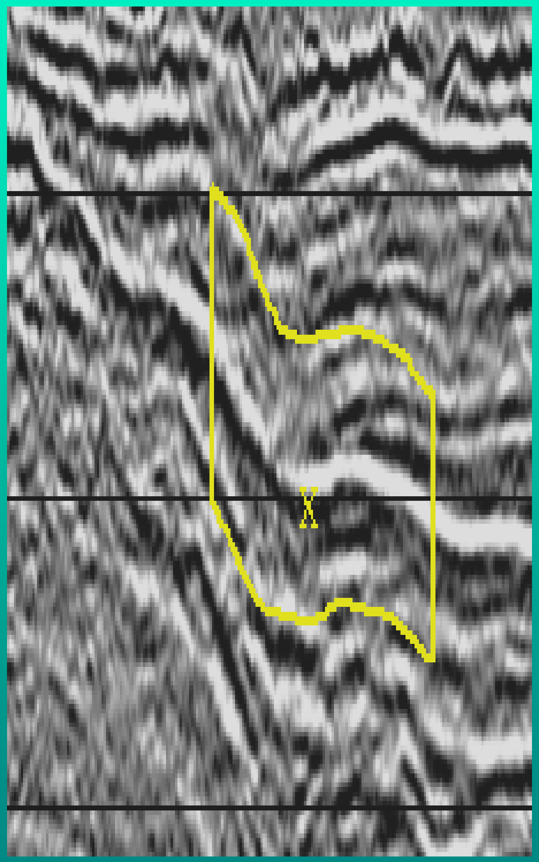

Dip-steered for flexible bodie

D

Figure 4, Comparison of "chimney" output (A) with that of "similarity" or "coherency" only attribute (B)

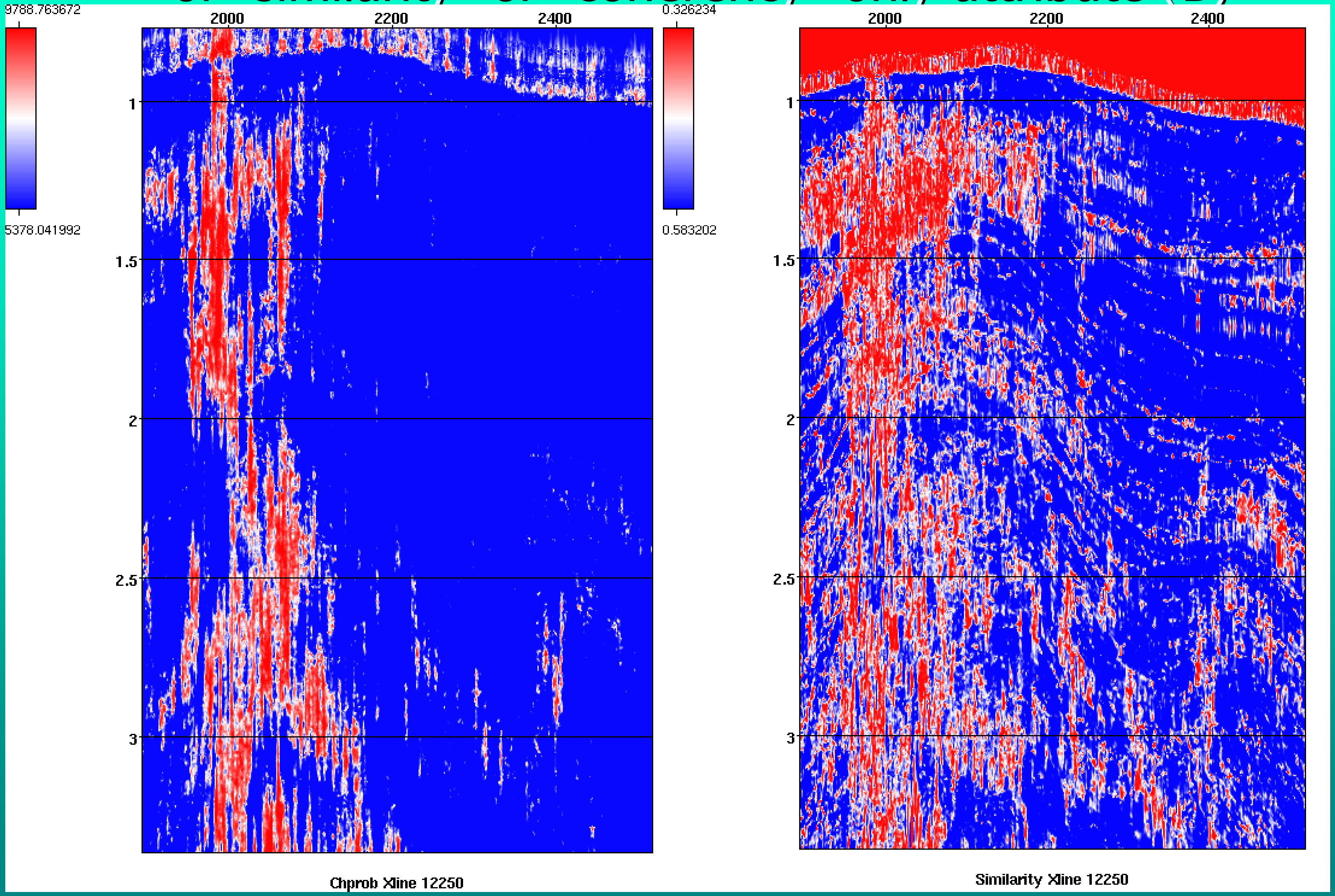

A

B

Figure 5- Non-linear mapping of all attributes through Fully connected Multi-Layer-Perceptron

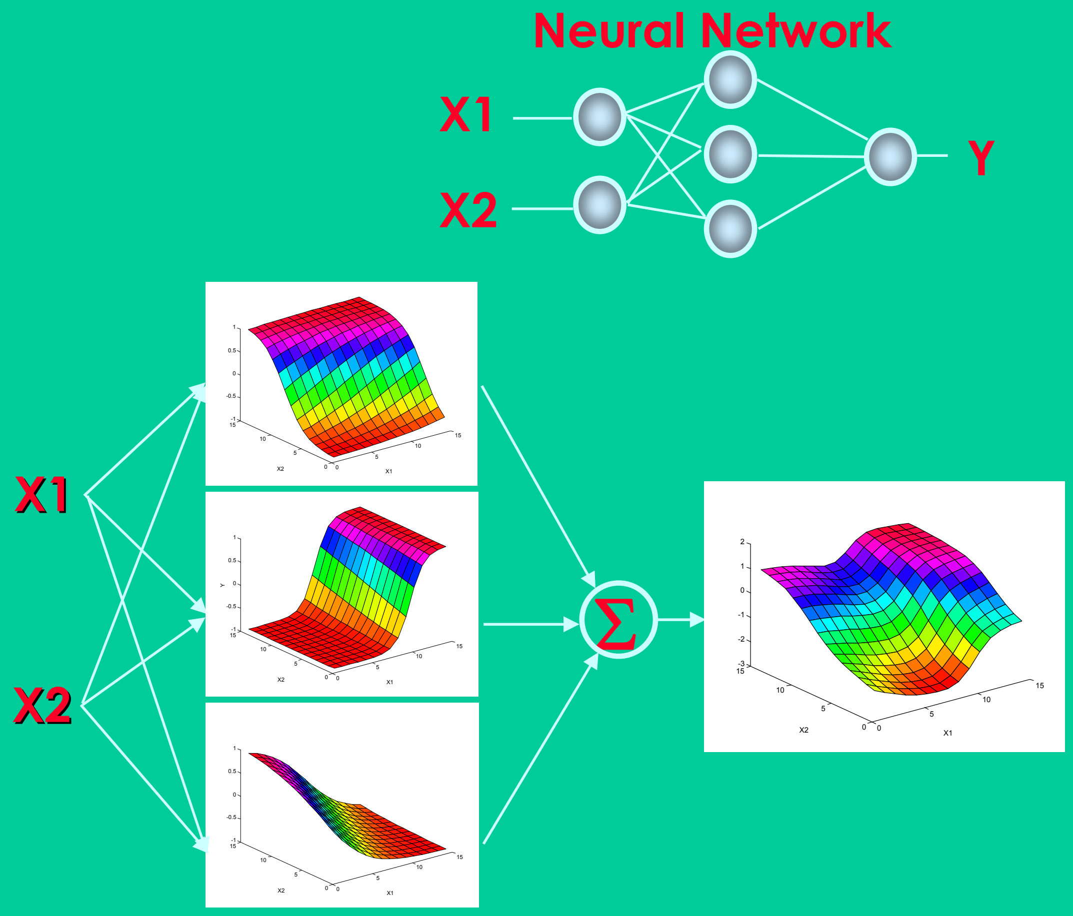

Figure 6- Structure of a neural network with different attributes calculated from the seismic data

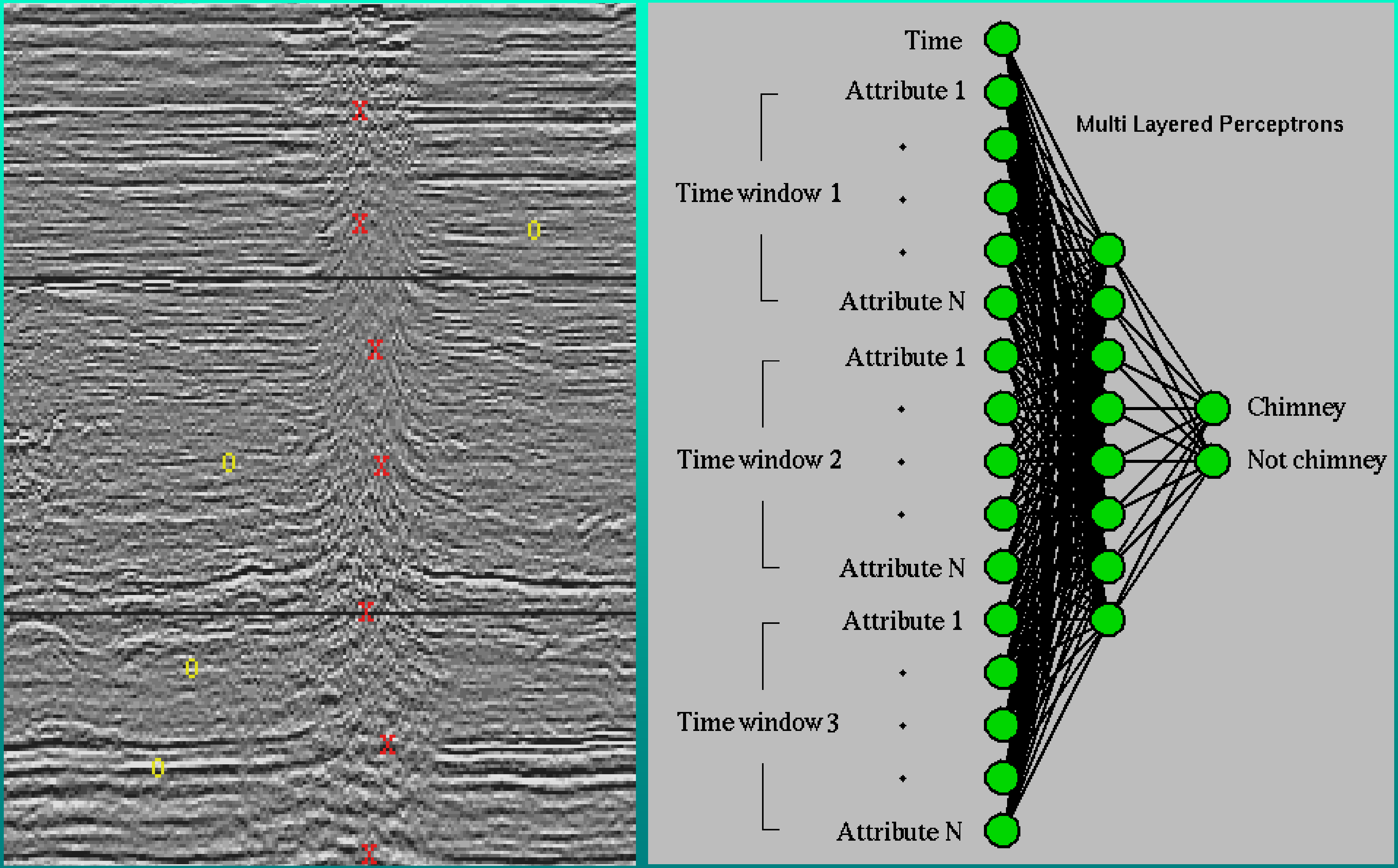

Figure 7, Neural network performance, (A) separation power attributes for chimneys and non-chimneys, (B) Convergence during the training, (C) Correct classification matrix

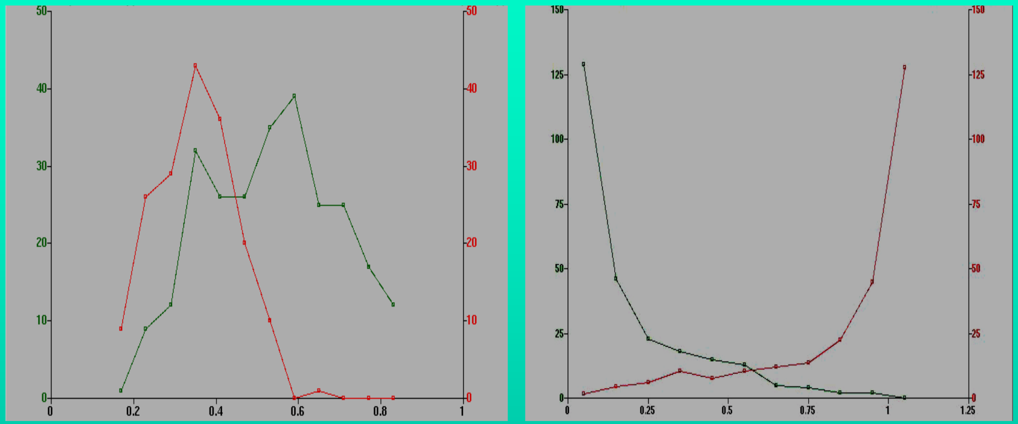

A

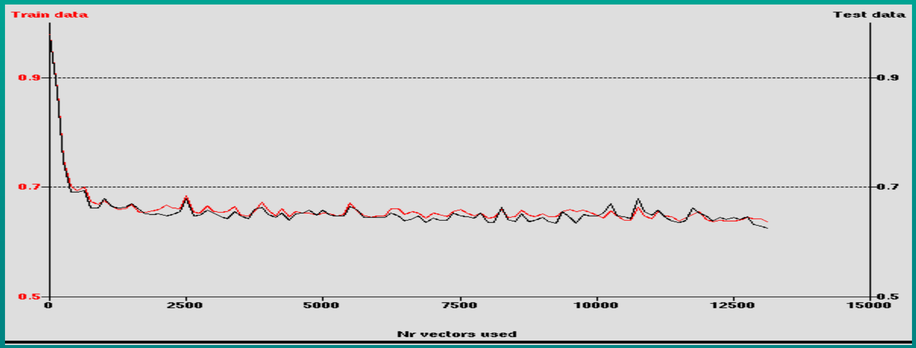

B

chimney	non- chimney	predicted / real
45%	5%	50% chimney
6%	44%	50% non-chimney
51%	49%	

C

Figure 8- Visualization of Chimneys with the structure.

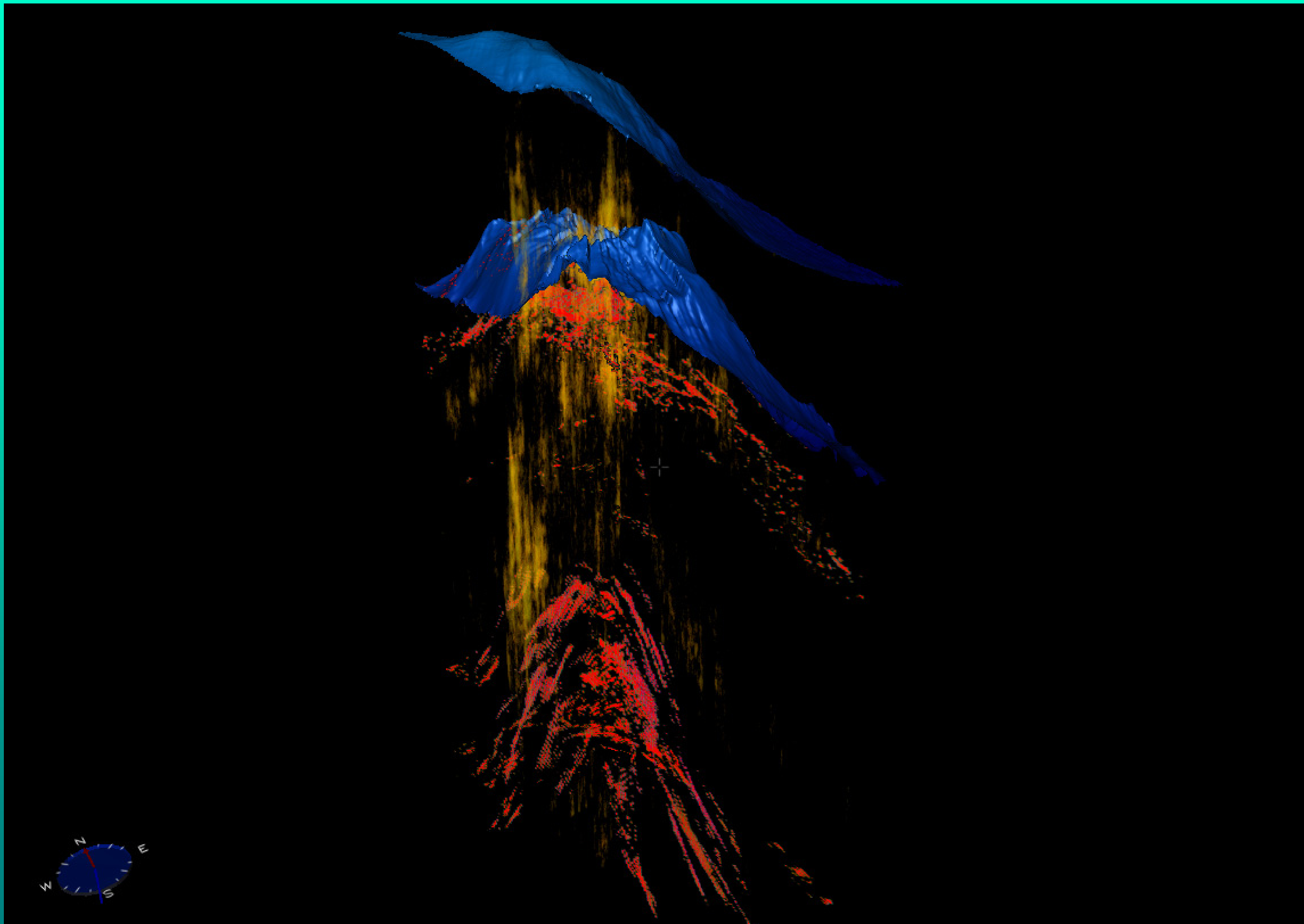

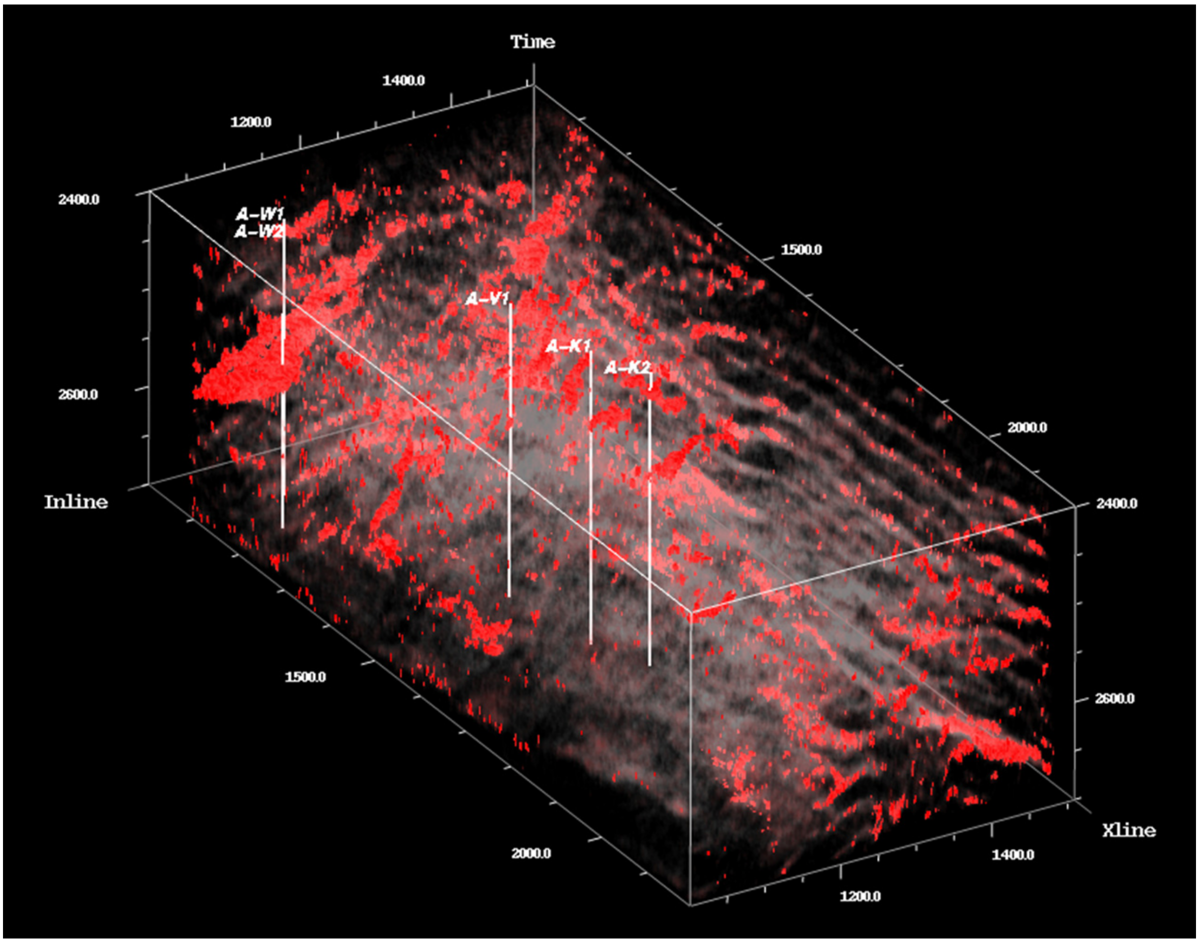

Figure 9 3-D view of Ibhubesi Field reservoir interval

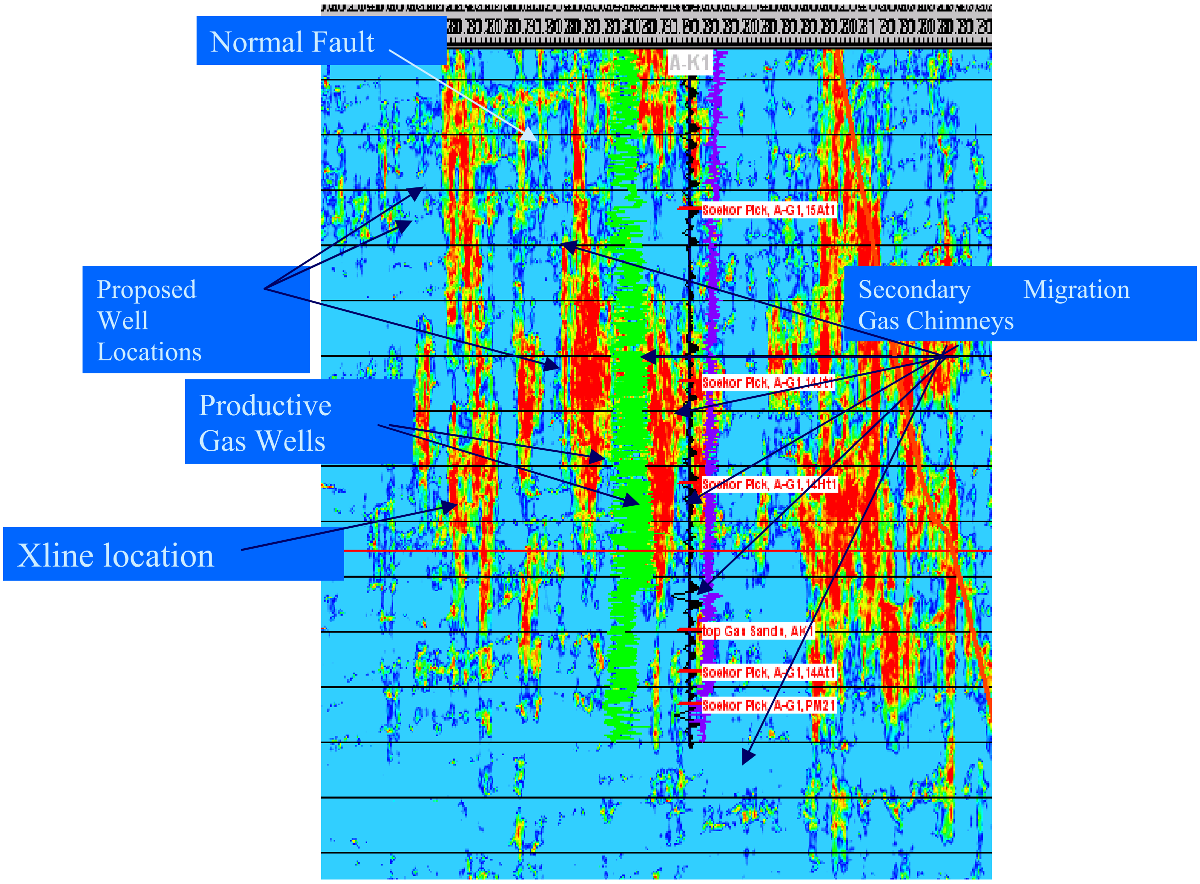

Figure 10, Secondary migration of gas

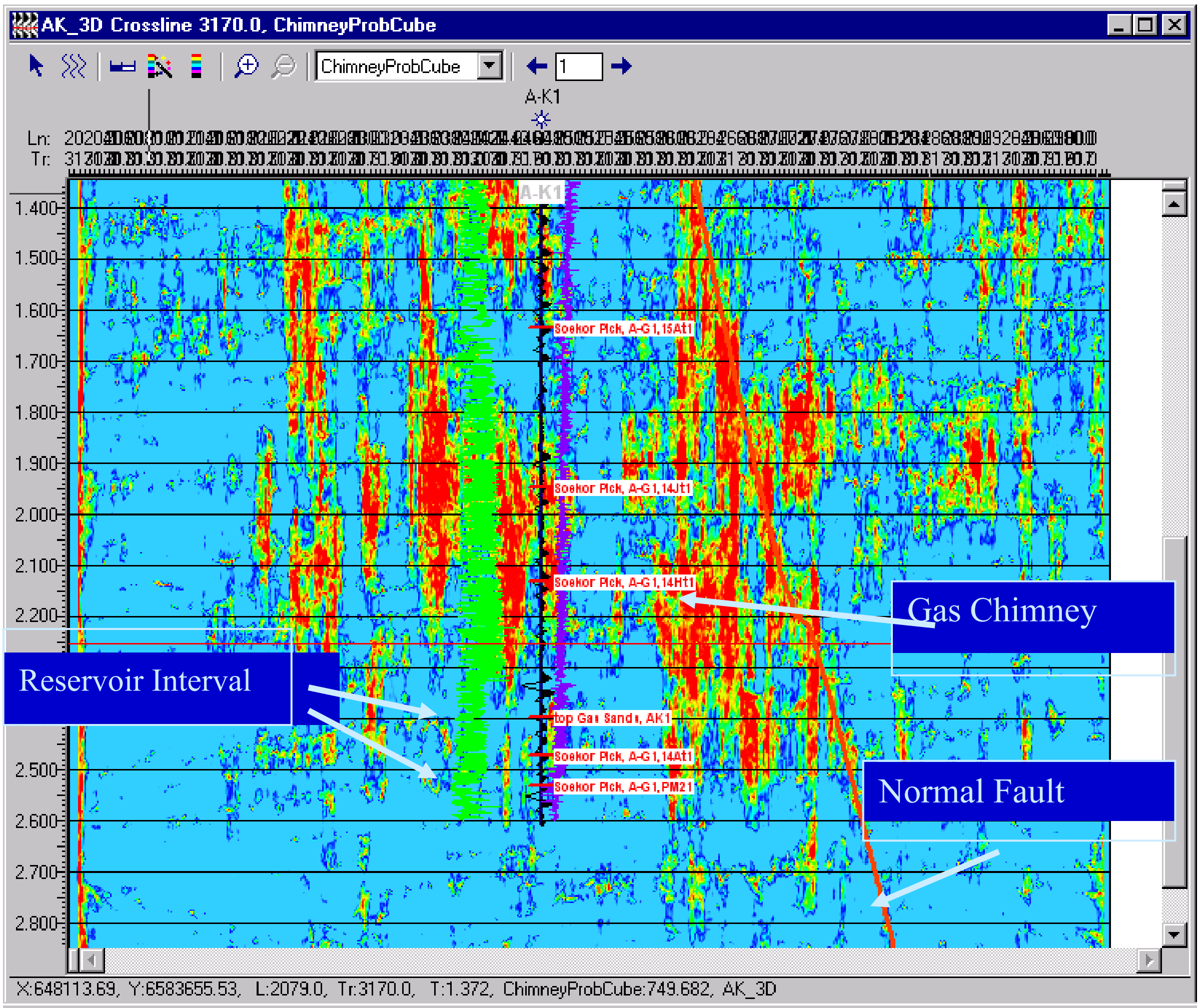

Figure 11 ertical Section: Gs seepage anomalies (red streaks) are seen originating at the reservoir level and ascending

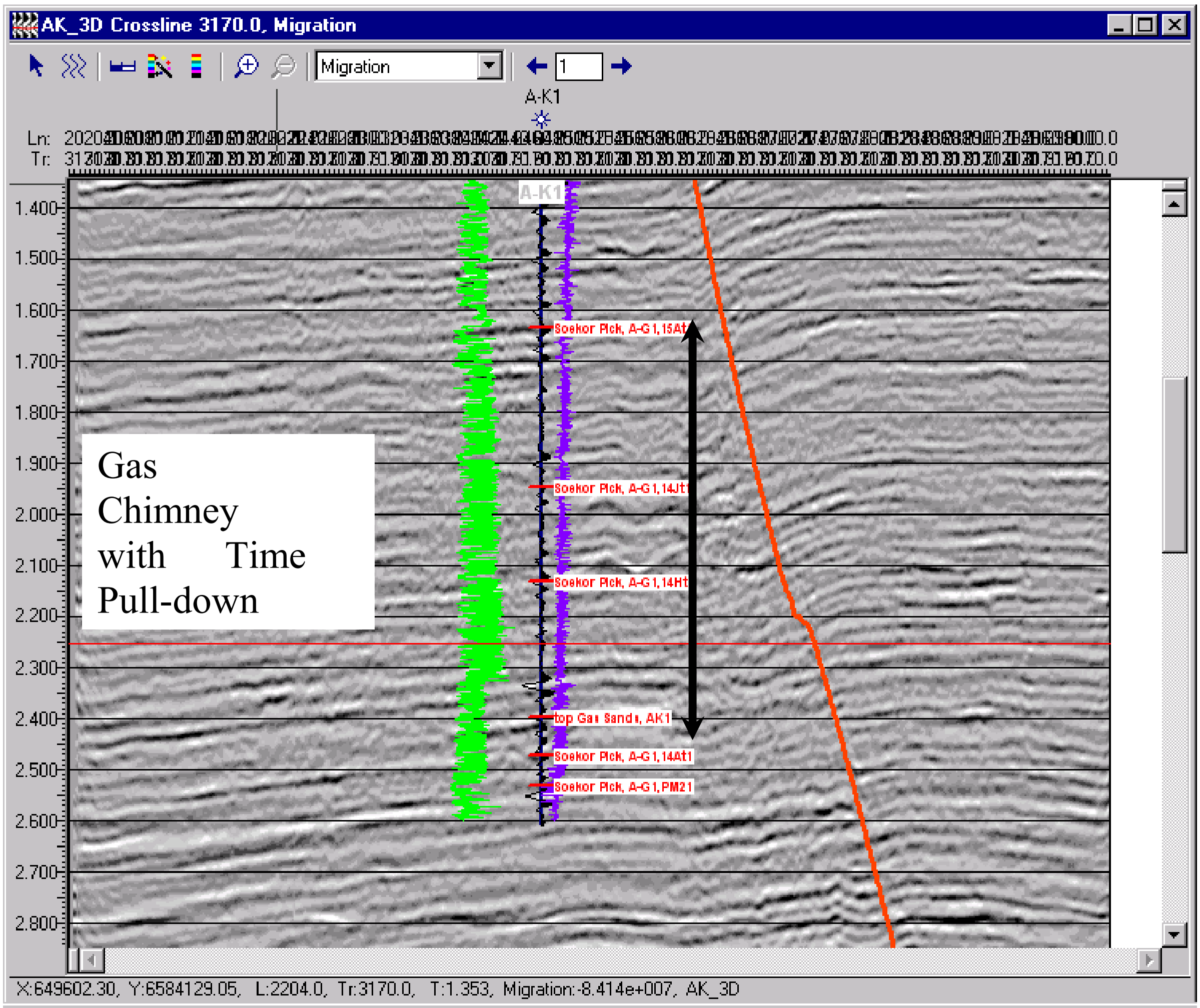

Figure 12, Conventional seismic display s showing gas chimney with a time pull-down (along arrow)

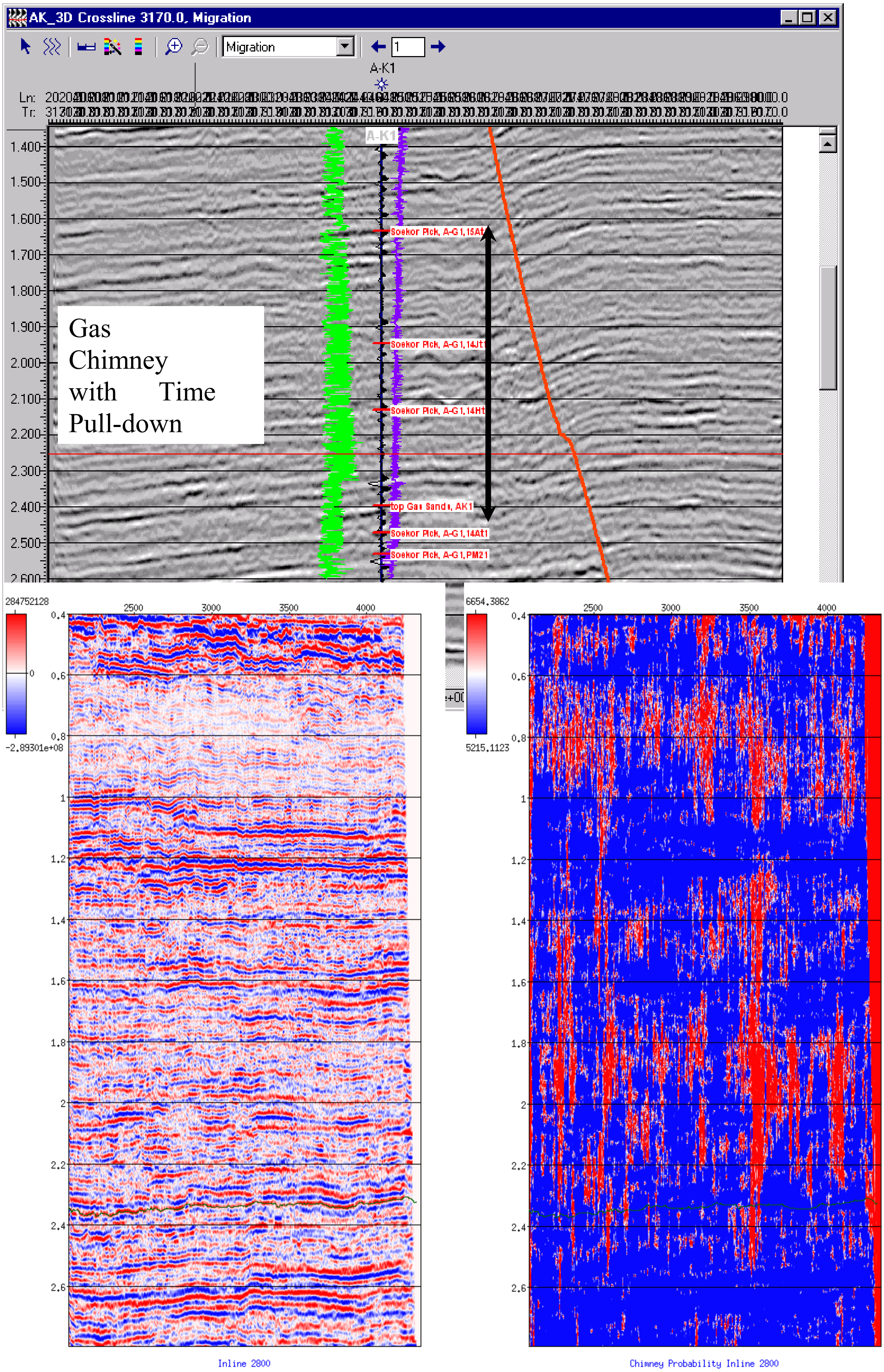
AK_3D Crossline 3170.0, Migration
Migration
A-K1
Gas Chimney with Time Pull-down
Soekor Pick, A-G1,15At
Soekor Pick, A-G1,14Jt1
Soekor Pick, A-G1,14Ht
top Gas Sands, AK1
Soekor Pick, A-G1,14At1
Soekor Pick, A-G1,PM21
284752128
-2.89301e+08
6654.3862
5215.1123
Inline 2800
Chimney Probability Inline 2800

Figure 13 Part of seismic inline 2800: input (left) neural network chimney prediction (right)

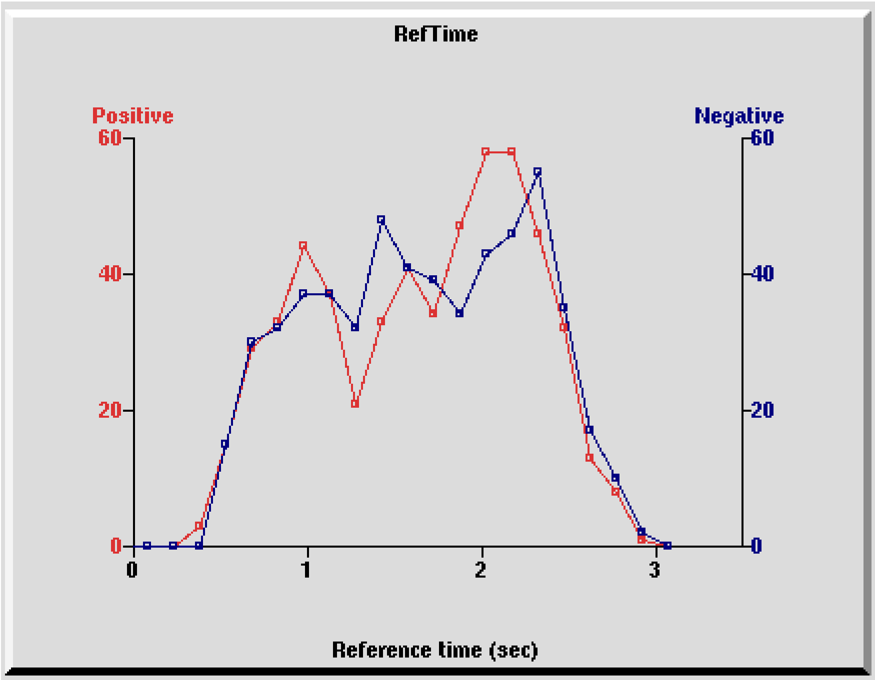

Figure 14 Distribution of selected training locations (positive and negative picks) over time-depth.

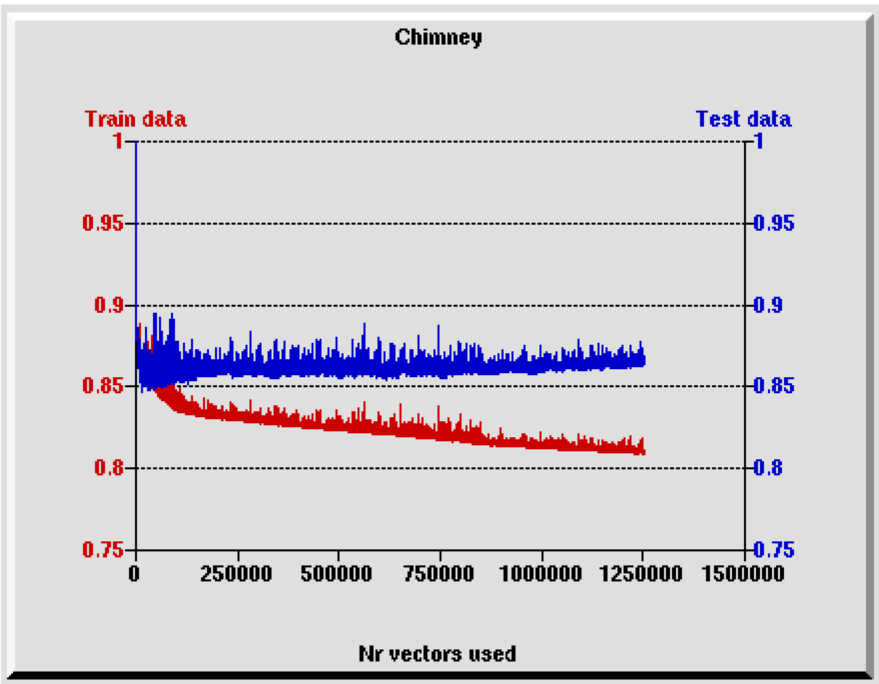

Figure 15 Neural network RMS error for the training and test set versus training cycles.

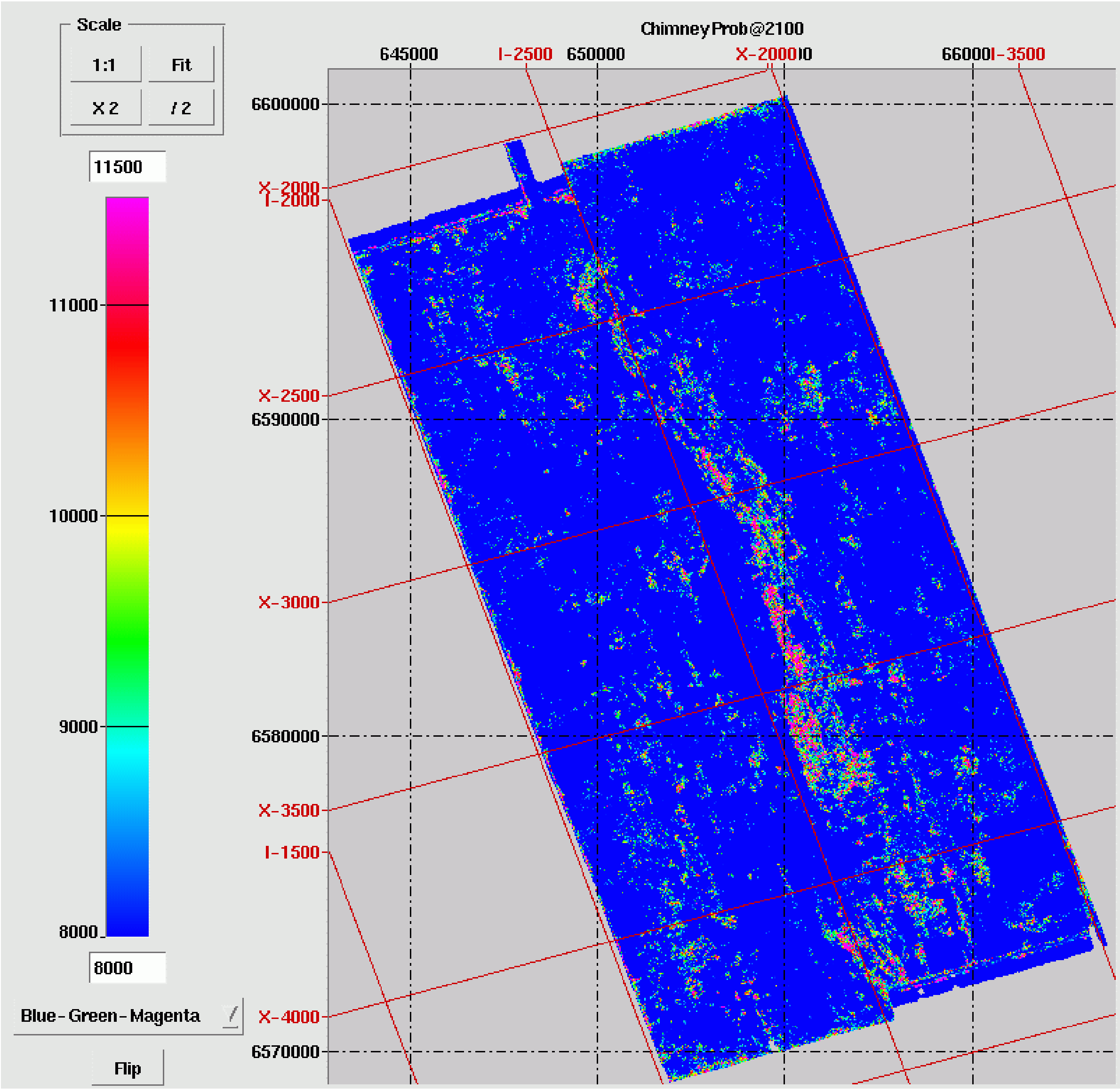

Figure 16 Neural network chimney prediction at 2100 ms

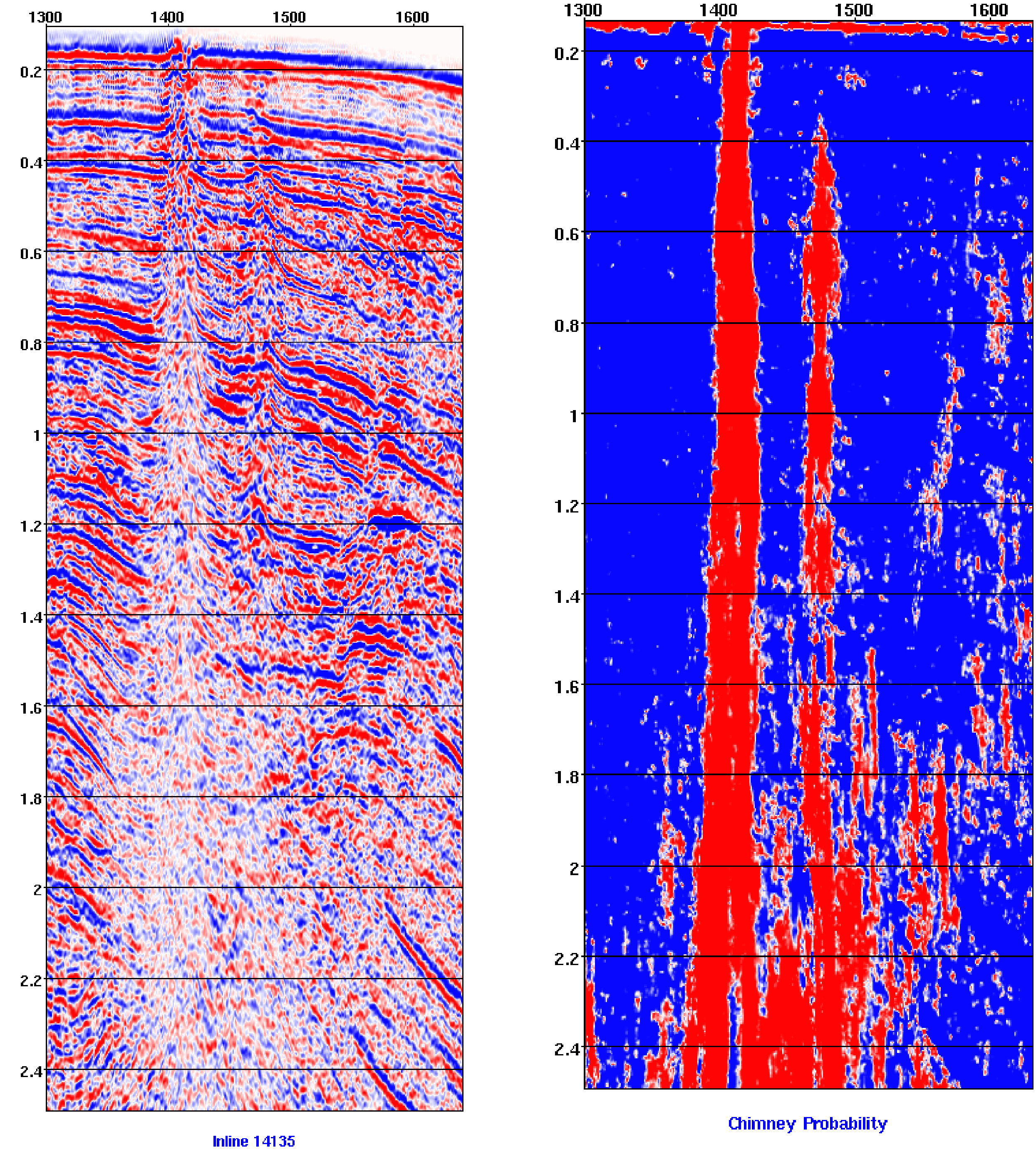

(a) (b)

Figure 17 Portion of an inline seismic section: input (left) neural network chimney prediction (right)

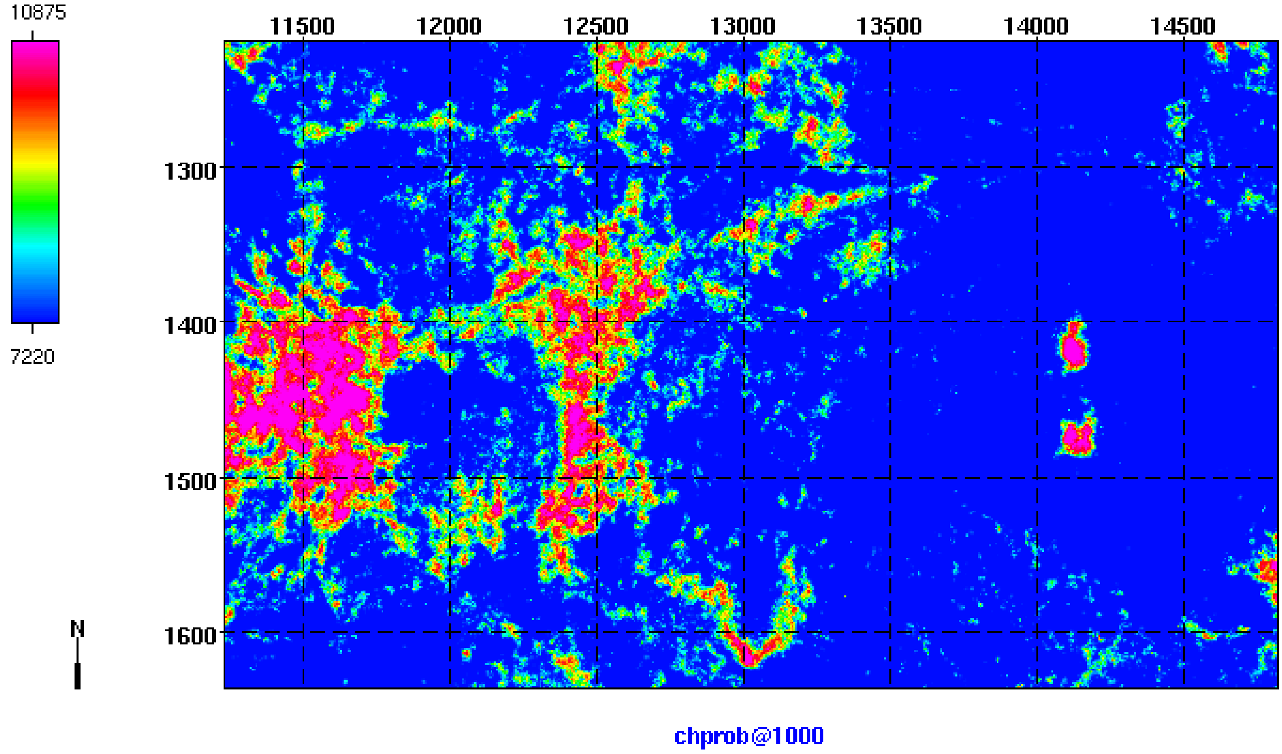

Figure 18 Neural network chimney prediction at 1000 ms

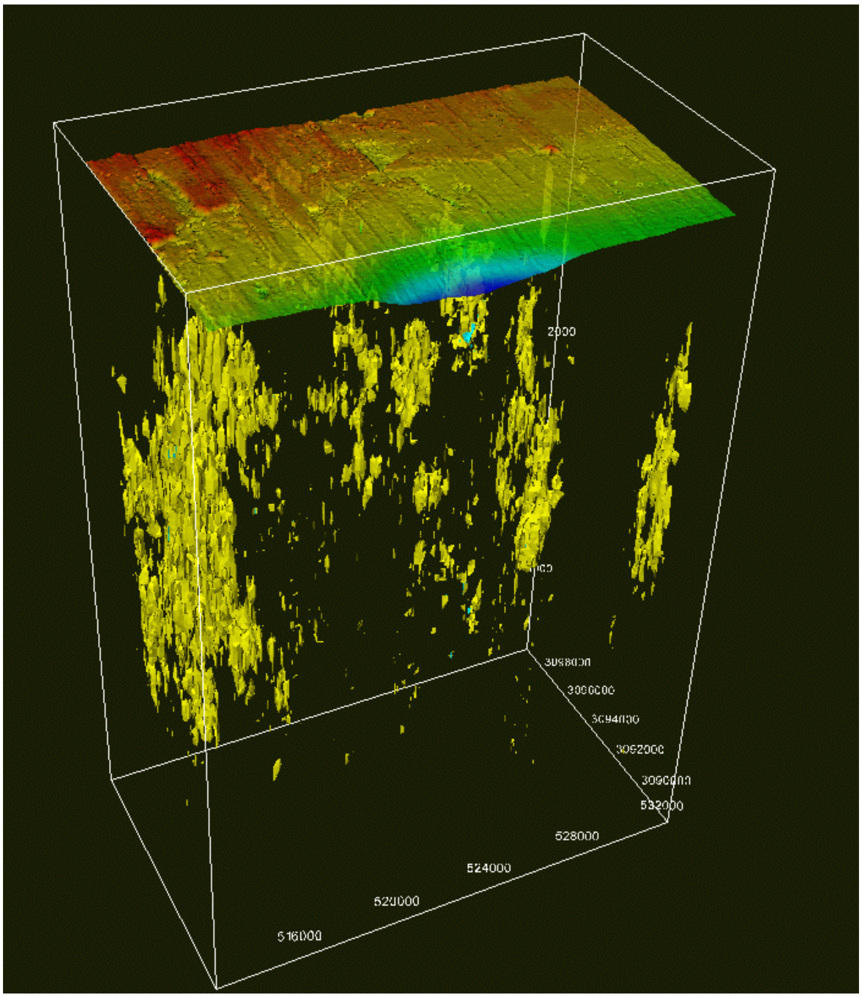

Figure 19 (A) 3D display of the Chimney Cube in the Gulf of Mexico.

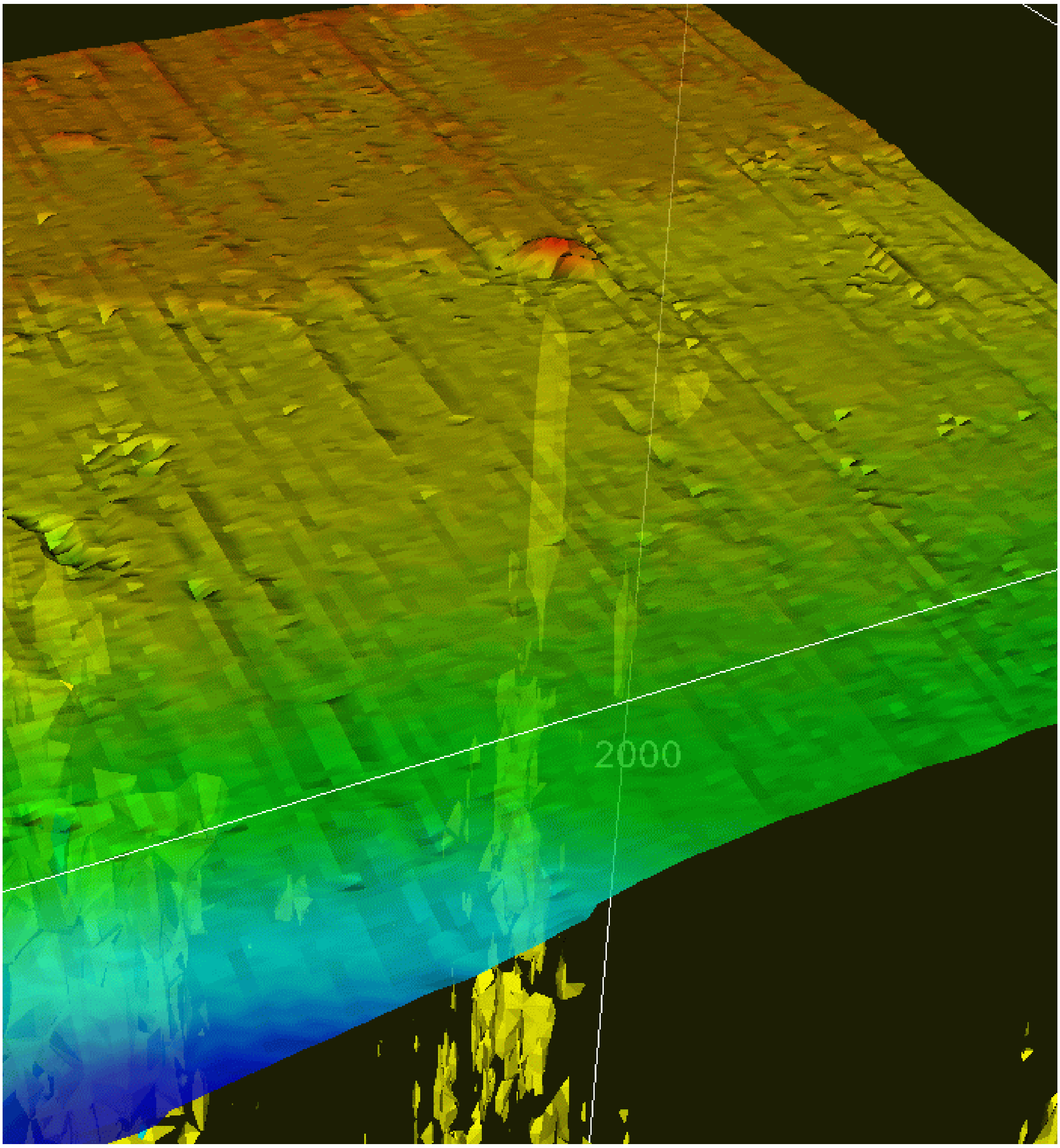

Figure 19(B) 3D detailed display of possible mud volcano at the sea bottom in relation with a chimney.